Chemical Geology 324–325 (2012) 87–98

Contents lists available at SciVerse ScienceDirect

Chemical Geology

journal homepage: www.elsevier.com/locate/chemgeo

Research paper

Anomalous molybdenum isotope trends in Upper Pennsylvanian euxinic facies: Significance for use of δ^{98}Mo as a global marine redox proxy

Achim D. Herrmann [a,*], Brian Kendall [b,f], Thomas J. Algeo [c], Gwyneth W. Gordon [b],
Laura E. Wasylenki [d], Ariel D. Anbar [e]

[a] Barrett, the Honors College and School of Earth and Space Exploration, Arizona State University, Tempe, AZ 85287-1612, United States
[b] School of Earth and Space Exploration, Arizona State University, Tempe, AZ 85287, United States
[c] Department of Geology, University of Cincinnati, Cincinnati, OH 45221-0013, United States
[d] Department of Geological Sciences, Indiana University, Bloomington, IN 47405-1405, United States
[e] School of Earth and Space Exploration and Dept. of Chemistry & Biochemistry, Arizona State University, Tempe, AZ 85287, United States
[f] Department of Earth & Environmental Sciences, University of Waterloo, 200 University Avenue West, Waterloo, Ontario, Canada N2L 3G1

ARTICLE INFO

Article history:
Accepted 20 May 2012
Available online 29 May 2012

Editor: J.D. Blum

Keywords:
Cyclothem
Black shale
Swope Formation
Superestuarine circulation
Epeiric sea
Hushpuckney Shale

ABSTRACT

The use of molybdenum isotope data (δ^{98}Mo) from organic-rich shales to draw inferences concerning marine paleoredox conditions at a global scale is predicated upon the assumptions of (1) a residence time of Mo in seawater much greater than the ocean mixing time, and (2) quantitative removal of Mo from a strongly euxinic ($[H_2S]_{aq} > 11$ μM) water column to the sediment, thus preserving the seawater δ^{98}Mo signature. In this study we analyze Mo isotopic variation in the Hushpuckney Shale, a 73-cm-thick unit representing the late transgressive to early regressive stages of a glacio-eustatic cyclothem (Swope Formation) deposited in the Late Pennsylvanian Midcontinent Sea (LPMS) of North America. The Hushpuckney can be subdivided into four stratigraphic zones of distinctive geochemical character. Zones I and III, which accumulated under weakly euxinic conditions, acquired relatively high δ^{98}Mo values (+0.9 to +1.1‰), whereas Zone II, which accumulated under intensely euxinic conditions, acquired lower δ^{98}Mo values (~+0.6‰). Zone IV, which accumulated under suboxic conditions in the water column, acquired the heaviest δ^{98}Mo values (+1.1 to +1.8‰). These results contrast with the pattern of redox – δ^{98}Mo covariation in modern marine environments, in which the heaviest δ^{98}Mo values are found in the most intensely euxinic facies.

We evaluate three different hypotheses to account for the Mo isotopic patterns of the Hushpuckney Shale. One hypothesis, seawater–freshwater mixing, is rejected owing to isotopic mass balance considerations. A second hypothesis is a local control on δ^{98}Mo by water-column redox cycling of Mn, with particulate Mn-oxyhydroxides adsorbing isotopically light Mo and transferring it to the sediment, a process that was most active during deposition of Zone II. The significance of this scenario is that euxinic black shales may not reliably record global seawater δ^{98}Mo in areas where a Mn-particulate shuttle is operative. A third hypothesis is based on rapid secular variation of the Mo isotope composition of Late Pennsylvanian global seawater. In order to account for δ^{98}Mo trends within the Hushpuckney Shale, seawater δ^{98}Mo must have varied by ~1.2‰ at a ~100-kyr timescale, which would have been possible only if the residence time of Mo in Late Pennsylvanian seawater was <100 kyr. Although both the second and third hypotheses are viable based on the present limited δ^{98}Mo dataset, we discuss how each model might be tested through additional Mo isotope data.

1. Introduction

The molybdenum (Mo) isotope system has been extensively studied as a potential proxy for global ocean redox conditions (Barling et al., 2001; Siebert et al., 2003; Arnold et al., 2004; Poulson et al., 2006; Siebert et al., 2006; Lehmann et al., 2007; Neubert et al., 2008; Pearce et al., 2008; Wille et al., 2008; Gordon et al., 2009; Kendall et al., 2009; Poulson Brucker et al., 2009; Dahl et al., 2010a,b; Duan et al., 2010; Scheiderich et al., 2010a,b; Kendall et al., 2011; Neubert et al., 2011). The rate and completeness of removal of Mo to the sediment differs among (1) oxic ($[O_2]_{aq} > 10$ μM), (2) suboxic to weakly euxinic ($[O_2]_{aq} < 10$ μM, $[H_2S]_{aq} < 11$ μM), and (3) strongly euxinic ($[H_2S]_{aq} > 11$ μM) water-column redox facies. In oxygenated seawater, Mo is present as the largely unreactive molybdate anion (MoO_4^{2-}), which is removed slowly through adsorption to ferromanganese crusts. Adsorbed Mo has a light isotopic composition (~−0.7‰), representing a large (~3‰) negative fractionation relative to the modern seawater composition ($\delta^{98}Mo_{sw}$) of ~+2.3‰ (Barling et al., 2001; Siebert et al., 2003;

---

* Corresponding author.
E-mail address: achim@asu.edu (A.D. Herrmann).

0009-2541/$ – see front matter © 2012 Elsevier B.V. All rights reserved.
doi:10.1016/j.chemgeo.2012.05.013

Poulson Brucker et al., 2009). In anoxic seawater and pore fluids, Mo is converted to the particle-reactive thiomolybdate anion ($MoO_xS_{4-x}^{2-}$, x = 0 to 3), which is scavenged by organic matter and Fe-Mn particulates (Helz et al., 1996; Erickson and Helz, 2000; Zheng et al., 2000) or precipitated as a nanoscale Mo(VI)-Fe(II) sulfide mineral (Helz et al., 2011). In strongly euxinic watermasses such as below 400 m in the modern Black Sea, molybdate is converted to tetrathiomolybdate (MoS_4^{2-}) and removed quantitatively (i.e., completely) to the sediment, yielding a sediment Mo isotope signature close to that of seawater (Barling et al., 2001; Arnold et al., 2004; Neubert et al., 2008). If bottom waters are strongly euxinic but tetrathiomolybdate is not quantitatively removed, there may be a small fractionation of ~0.5‰ (Nägler et al., 2011). In suboxic and weakly euxinic facies, the removal of Mo from bottom waters is not quantitative, and isotopic fractionation associated with particle scavenging or equilibrium precipitation yields sediment δ^{98}Mo intermediate between that of Fe-Mn crusts and highly euxinic sediments (Arnold et al., 2004; Nägler et al., 2005; Poulson et al., 2006; Siebert et al., 2006; Neubert et al., 2008; Poulson Brucker et al., 2009).

The utility of Mo isotopes for analysis of global redox conditions depends on the residence time of Mo in seawater. Due to the long residence time of Mo in the modern ocean (~700–800 kyr, Millero, 1996; Morford and Emerson, 1999; or ~440 kyr, Miller et al., 2011), seawater δ^{98}Mo is globally uniform (~2.3‰; Barling et al., 2001; Siebert et al., 2003). Therefore, measurements from a single site can theoretically be used to infer the global extent of oxic versus suboxic/weakly euxinic versus strongly euxinic sinks of seawater Mo (Barling et al., 2001; Arnold et al., 2004; Neubert et al., 2008; Kendall et al., 2009, 2011; Dahl et al., 2010b). However, this approach would not be viable if the residence time of Mo in seawater were considerably shorter than at present (e.g., Algeo, 2004) or if the renewal time of bottom waters in restricted marine basins were long relative to that residence time. The renewal time of ancient restricted watermasses can be evaluated using recently developed geochemical approaches (Algeo and Lyons, 2006; Algeo and Rowe, 2012).

The extent of marine euxinic facies expanded greatly during interglacial stages of the Late Paleozoic Ice Age, when melting of continental icesheets in the Southern Hemisphere caused global sea-level elevations to rise by ~60–150 m, flooding the interiors of North America and other cratons (Heckel, 1994; Joachimski et al., 2006). At its maximum extent, the Late Paleozoic Midcontinent Sea (LPMS) of North America covered an area of ~2.1×10^6 km^2, making it larger than modern epicontinental seas such as Hudson Bay and the Baltic Sea (Fig. 1; Algeo et al., 2008a). Whereas these modern seas have either permanently or intermittently oxic bottom waters, LPMS deep waters went anoxic for extended intervals (possibly ~100 kyr; Algeo and Heckel, 2008), resulting in the deposition of laminated, organic-rich black shales (Algeo et al., 2004; Heckel, 2008). These offshore (or "core") shales are thin (<1 m) but laterally extensive, some being traceable from Oklahoma and Kansas northeastward to Iowa and Illinois (Heckel, 1977; Watney et al., 1995), and probably correlative with similar organic-rich shales in eastern Europe (Heckel et al., 2007). The black shale intervals are characterized by abundant phosphatic granule layers, a lack of biota other than nektonic and planktic organisms, strongly ^{34}S-depleted authigenic sulfides, and a high degree of pyritization (DOP) (Coveney et al., 1991; Schultz and Coveney, 1992; Algeo et al., 2008b). These features are thought to reflect slow accumulation in a sediment-starved, distal offshore setting with oxygen-depleted, sulfidic bottom waters.

Herein, we report Mo abundance and isotope data from the Hushpuckney Shale of the Upper Pennsylvanian Swope Formation from eastern Kansas. This interval has been the subject of a number of earlier paleoceanographic studies (e.g., Hoffman et al., 1998; Cruse and Lyons, 2000; Algeo et al., 2004, 2008a, 2008b; Algeo and Heckel, 2008) that can be used to help interpret the Mo isotope record of the present study. Algeo et al. (2008a) estimated that the residence time of seawater within the LPMS was ~70–130 years, which is shorter than that of the deep watermass of the modern Black Sea (~400–800 years; Algeo and Lyons, 2006; Algeo and Rowe, 2012). Thus, the Mo isotope composition of the Hushpuckney Shale might be expected to reflect contemporaneous global seawater δ^{98}Mo in the same manner in which the euxinic facies of the Black Sea reflects modern seawater δ^{98}Mo. However, the Hushpuckney Shale yielded a redox-δ^{98}Mo relationship opposite that observed in the Black Sea and other modern marine systems, leading us to develop a number of hypotheses to explain the anomalous patterns in our study unit.

2. Paleogeographic setting and sequence stratigraphy of the Hushpuckney Shale

2.1. Paleogeographic, paleoclimatic, and paleohydrologic setting

The LPMS (Fig. 1) was a geographically enclosed sea, surrounded by young mountain belts to the south, the Laurentian craton to the east and north, and the Ancestral Rocky Mountains to the west (Algeo and Heckel, 2008; Algeo et al., 2008a). Lithofacies associations in Wyoming indicate that shallow-marine facies (e.g., evaporitic lagoons) or subaerial exposure (e.g., migrating dune fields) prevailed in this region. The only significant connection of the LPMS to the open ocean was a deepwater passage through the Permian Basin Seaway (Fig. 1). There was no sill between the open ocean and the LPMS that would have led to a watermass restriction similar to the modern Black Sea. The water balance of this epicontinental sea was driven by the advection of deep open-ocean water through the Permian Seaway and the tropical, humid climate of the equatorial belt (Schutter and Heckel, 1985; Crowley et al., 1989, 1996; Poulsen et al., 2007; Horton and Poulsen, 2009; Horton et al., 2010).

An estimated ~800–1500 km^3 of freshwater flowed into the LPMS each year (Algeo and Heckel, 2008; Algeo et al., 2008a). When normalized to drainage area, this is approximately equivalent to the freshwater influx to the modern Hudson Bay (~975 km^3 y^{-1}) and the Baltic Sea (~485 km^3 y^{-1}) (Algeo et al., 2008a). Given the size of the basin and the general ocean circulation pattern of the LPMS, the estimated residence time of seawater within the LPMS was approximately ~70–130 years.

The enclosed paleogeographic setting, with a western connection to the open ocean and focused freshwater input from continental runoff in the east, likely led to the development of an extensive freshwater lens and the establishment of a strong pycnocline (Algeo et al., 2004; Algeo and Heckel, 2008). Algeo and Heckel (2008) hypothesized that the benthic anoxic conditions of the black shale intervals were driven by the lateral advection of oxygen-depleted Panthalassic intermediate waters through the Permian Basin Seaway underneath this strong pycnocline. The strength of this pycnocline varied spatially (with distance from the shoreline) and temporally (with changes in freshwater input as a function of varying climatic humidity during cyclothem deposition), resulting in geochemical gradients across the LPMS (Hoffman et al., 1998; Algeo and Heckel, 2008).

Despite the nearly landlocked paleogeographic setting of the LPMS, its deep watermass is thought to have exchanged freely with global seawater. First, high trace metal/TOC ratios and strong positive covariation of trace-metal concentrations in cyclothemic black shales are indicative of a deep watermass that has an undepleted and stable inventory of dissolved trace metals, which is generally the case only for open-ocean seawater (Algeo and Maynard, 2008). Second, nitrogen isotopic patterns in cyclothemic black shales are most readily explained through lateral advection of ^{15}N-depleted intermediate watermasses from the eastern tropical Panthalassic Ocean, a process that would have been possible only in the case of unrestricted deepwater circulation (Algeo et al., 2008b). In the Hushpuckney Shale, the positive excursion of δ^{15}N to a maximum of ~+14‰ reflects the incursion of denitrified, oxygen-deficient open-ocean seawater during the transgressive stage of the Swope Formation cyclothem (Algeo et al., 2008b). Deepwater exchange took place through a deep corridor extending through the Greater Permian Basin region that was carved during Late Pennsylvanian glacio-eustatic lowstands (Algeo et al., 2008a).

2.2. Sequence stratigraphic and depositional model of Pennsylvanian core shales

The general model for the deposition of Pennsylvanian cyclothems is linked to glacio-eustatic cycles of the Late Paleozoic Ice Age (Greb et al., 2008; Heckel, 1986, 2008). In this model, deglaciation of Gondwanan ice sheets resulted in global sea-level rise and flooding of low-lying cratonic interiors. During the initial transgression, shallow-water limestones accumulated on top of terrestrial deposits (commonly paleosols). As sea level continued to rise, limestone deposition ceased and dark gray to black organic-rich shales accumulated. The accumulation of large quantities of organic matter in the latter units is linked to humid and warm climate conditions during sea-level highstands (Algeo et al., 2004). Strong runoff produced an extensive freshwater lens, yielding a quasi-estuarine circulation pattern within the LPMS and the development of a strong pycnocline (Algeo and Heckel, 2008; Algeo et al., 2008a). As global climate started to cool and Gondwanan ice sheets began to grow again, sea level fell and climate conditions became increasingly arid, resulting in reduced runoff and weaker stratification of the LPMS water column (Algeo et al., 2004). Black shale deposition ceased and gray shales accumulated instead. In sequence stratigraphic terms, the black shale facies of cyclothemic core shales represents the late transgressive through highstand systems tracts, while the gray shale facies represents the early regressive systems tract.

3. Methods

3.1. Sample description

We collected samples from both the black shale and gray shale facies of the Hushpuckney Shale of the Swope Formation in the Kansas Geological Survey Orville Edmonds No. 1A drillcore. High DOP$_{\text{est}}$ values (0.60–0.80) indicate that the black shale facies was deposited under anoxic and sulfidic (euxinic) conditions below the pycnocline. Lower DOP$_{\text{est}}$ values (0.35–0.50) indicate that the gray shale facies was deposited under suboxic conditions, probably within the chemocline that separated oxygenated surface waters from euxinic deep waters (Heckel, 1977; Algeo and Maynard, 2004; Cruse and Lyons, 2004; Algeo et al., 2008b). Other aspects of the geochemistry of the same study unit were investigated in earlier studies (Hoffman et al., 1998; Algeo et al., 2004, 2008b; Algeo and Tribovillard, 2009).

3.2. Mo isotope geochemistry

Mo abundance and isotope data were obtained at the W.M. Keck Foundation Laboratory for Environmental Biogeochemistry, School of Earth and Space Exploration, Arizona State University. Approximately 0.1 g of powdered sample was ashed overnight at 550 °C and dissolved completely by standard HF-HNO$_3$-HCl digestion. An aliquot of the sample digest equivalent to 250 ng of Mo was appropriately spiked with a calibrated ^{97}Mo–^{100}Mo double spike and purified through anion and cation exchange chromatography (Gordon et al., 2009; Dahl et al., 2010a). Samples were analyzed on a Thermo Scientific Neptune MC-ICP-MS with an Apex sample introduction system. In the absence of an

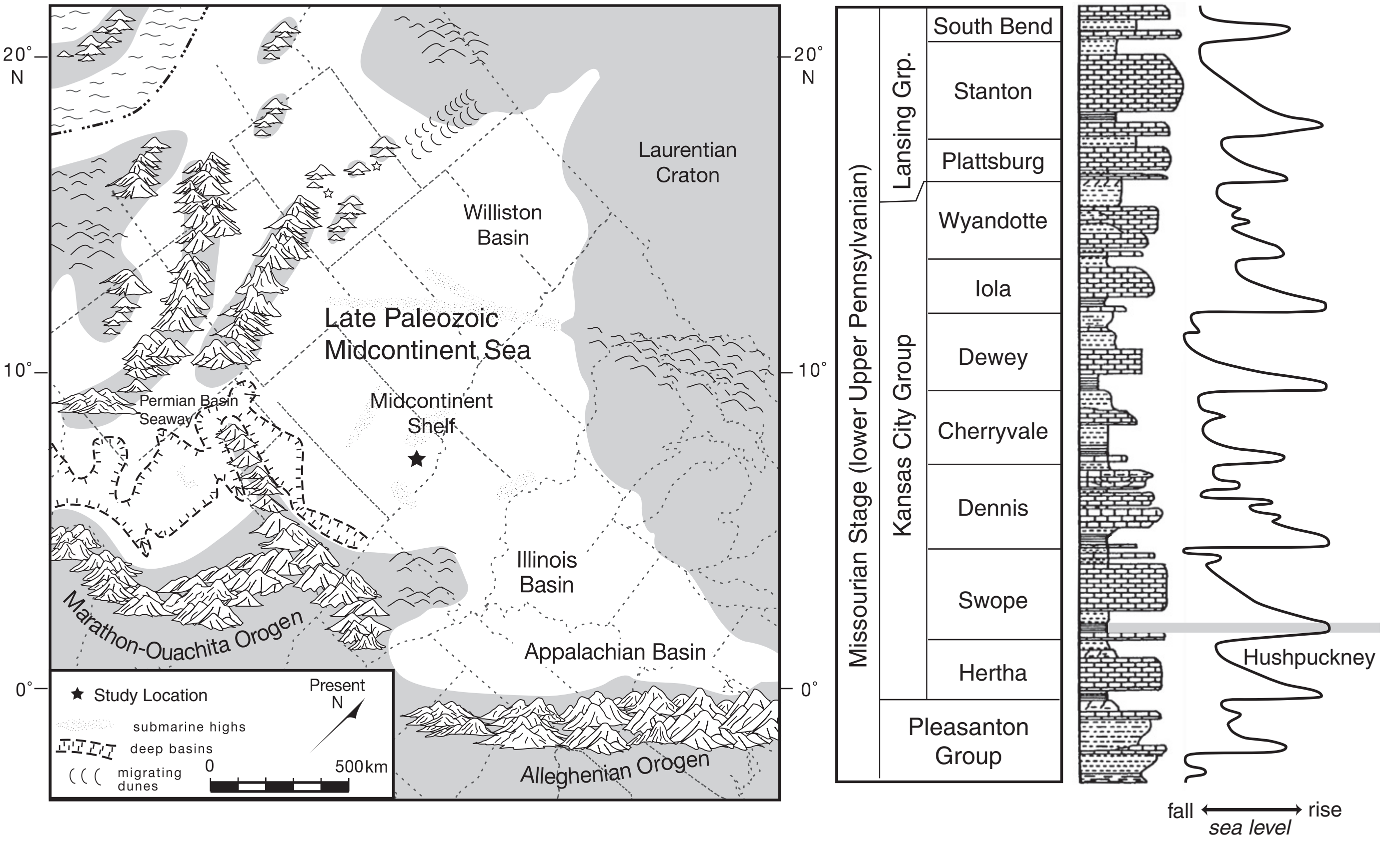

Fig. 1. Paleogeography of the Late Paleozoic Midcontinent Sea (based on Algeo et al., 2008a); Missourian Stage stratigraphy after Heckel (1977). The cyclic nature of the Late Pennsylvanian strata is generally interpreted a as far-field record of waxing and waning of Gondwanan icesheets (Greb et al., 2008; Heckel, 2008).

internationally accepted standard, we report our data as δ^{98}Mo relative to our in-house ICP standard (Johnson Matthey Specpure Lot #802309E):

$$\delta^{98}\mathrm{Mo}_{\mathrm{sample}}(‰) = \left[{}^{98/95}\mathrm{Mo}_{\mathrm{sample}}/{}^{98/95}\mathrm{Mo}_{\mathrm{standard}} - 1\right] \times 1000$$

The δ^{98}Mo value for modern seawater is 2.3 ± 0.1‰ on this standard scale (Barling et al., 2001). Based on replicate measurements of the same sample solutions, the external reproducibility was better than ±0.07‰ (±0.023‰/amu, 2 SD; Table 1 in online material). Five samples were ashed, digested, spiked and processed in duplicate, and the external reproducibility for the measured δ^{98}Mo values was between 0.01 and 0.08‰. Mo concentrations were determined by isotope dilution. Each sample was measured at least in triplicate, with a typical concentration reproducibility of around 0.02%. The Mo abundance data obtained through mass spectrometry matches within analytical uncertainty those obtained through XRF (Table 1 in online material).

4. Results

Mo concentrations in the Hushpuckney Shale range from ~25 ppm to ~700 ppm with a mean concentration of ~200 ppm (Fig. 2). These values are 1 to 3 orders of magnitude greater than that of average upper continental crust (~1.5 ppm; McLennan, 2001; Arnórsson and Óskarsson, 2007), indicating that nearly all the Mo in these shales is of authigenic origin and that their δ^{98}Mo values represent the isotopic composition of this authigenic fraction.

The study unit can be subdivided into four zones of relatively uniform geochemical character that correspond to natural sequence stratigraphic units (Fig. 2). Zones I to III represent the lower, middle, and upper parts of the black shale facies of the Hushpuckney Shale in the Edmonds #1A drillcore (Algeo et al., 2004). Zone I (0–7 cm) corresponds to the late transgressive stage of a Late Pennsylvanian glacio-eustatic cycle and overlies a thin limestone unit representing the onset of transgression. Zones II (7–26 cm) and III (26–43 cm) correspond to the early and late highstand stages of a glacio-eustatic cycle and are separated by the maximum flooding surface (MFS) at ~25 cm. Zone IV (43–73 cm) represents the gray shale facies of the Hushpuckney Shale, which was deposited during the early regressive stage of the glacio-eustatic cycle and is overlain by a thick limestone unit representing the late regressive stage.

These zones are characterized by markedly different Mo concentrations and isotopic compositions (Fig. 2). Zone I exhibits a sharp rise in Mo concentrations upsection from 36 ppm to 686 ppm despite nearly uniform δ^{98}Mo values of +0.89–0.95‰ (average +0.92‰). Zone II has the highest average Mo concentrations (average ~350 ppm; max. 608 ppm) and shows a rapid decline in δ^{98}Mo from +0.95‰ at 8 cm to +0.54‰ at 12 cm, followed by a slow increase upsection to +0.63‰ at 25 cm (average +0.62‰). Zone III exhibits a sharp decline in Mo concentrations (from ~280 ppm to ~50 ppm) and a concurrent increase in δ^{98}Mo to +0.89–1.09‰ (average +0.96‰). These trends continue into Zone IV, where Mo concentrations drop from 37 ppm to <10 ppm and δ^{98}Mo increases to +1.11–1.22‰ at 58–68 cm. The uppermost sample in the section (73 cm) yields both the lowest Mo concentration (9 ppm) and the highest δ^{98}Mo (+1.77‰; based on two replicate analyses).

The Mo isotope record covaries strongly with paleoredox and other geochemical proxies (Fig. 2). The $\mathrm{DOP}_{\mathrm{est}}$ profile indicates that euxinic conditions developed rapidly near the base of the black shale facies and intensified to the level of the MFS at ~25 cm (Fig. 2; Algeo et al., 2004, 2008b). Hence, the lightest δ^{98}Mo values in the Hushpuckney Shale (Zone II) correspond to the lowest benthic redox potentials. The pronounced shift towards heavier δ^{98}Mo values above 25 cm is associated with the transition from intensely euxinic conditions in Zone II to weakly euxinic conditions in Zone III (upper black shale facies) and then to suboxic conditions in Zone IV (gray shale facies) (Algeo et al., 2004). Although sediment δ^{98}Mo was not controlled directly by redox conditions (see Discussion), its inverse relationship to $\mathrm{DOP}_{\mathrm{est}}$ (Fig. 3) indicates that Mo isotopic variation in the Hushpuckney Shale was controlled by a process linked to benthic redox conditions.

A general pattern of negative covariation between Mo concentrations and δ^{98}Mo values might be inferred from a cursory inspection of the geochemical profiles in Fig. 2. In fact, a crossplot of Mo concentrations versus δ^{98}Mo suggests the existence of a more complex relationship between these proxies (Fig. 4). Zones I and III define a field characterized by relatively invariant δ^{98}Mo values (~+0.9–1.0‰) over a wide range of Mo concentrations. Zone II also exhibits limited δ^{98}Mo variation over a wide range of Mo concentrations, but it is characterized by markedly lower δ^{98}Mo values (~+0.5–0.7‰). Zone IV, representing the gray shale facies, exhibits a different pattern: uniformly low Mo concentrations (<40 ppm) but a much wider range of δ^{98}Mo values (~+1.1–1.8‰). The samples of Zones I, III and IV may define a continuum of [Mo]-δ^{98}Mo covariation characterized by a sharp rise in δ^{98}Mo at lower Mo concentrations (Trend 1), whereas Zone II samples record a shift toward lower δ^{98}Mo irrespective of the degree of authigenic Mo enrichment (Trend 2; Fig. 4).

The four zones identified above exhibit different distributions and Mo/TOC correlation slopes on a [Mo]-TOC crossplot (Fig. 5). Zone I shows a rapid increase in Mo with higher TOC values to peaks of ~686 ppm Mo and ~26% TOC, yielding a Mo/TOC slope of ~50 ppm/wt.% with a negative y-intercept. Zone II yields a slope of 9 ppm/wt.% with a positive y-intercept. Zone III shows reduced Mo and TOC values (max. ~280 ppm and 25%, respectively), yielding a slope of ~5 ppm/wt.% with a near-zero y-intercept. Zone IV exhibits sharply lower Mo and TOC values (max. ~40 ppm and 5%, respectively), yielding a slope of ~8 ppm/wt.% with a near-zero y-intercept. The slopes of Mo-TOC crossplots can be interpreted in terms of bottom water Mo concentrations (Algeo and Lyons, 2006; Algeo and Rowe, 2012).

The sample groups for Zones I to IV define a continuum on a $\mathrm{Mo}_{\mathrm{EF}}$–$\mathrm{U}_{\mathrm{EF}}$ crossplot (Fig. 6), rather than discrete fields as for Mo-TOC covariation (Fig. 5). The trend for the study section as a whole shows values that increase from a minimum of ~10 $\mathrm{Mo}_{\mathrm{EF}}$ and 1 U_{EF} to a maximum of ~200–300 for both $\mathrm{Mo}_{\mathrm{EF}}$ and U_{EF} (Fig. 6). Thus, as trace-metal concentrations increase, the rate of authigenic U enrichment rises more rapidly than that of authigenic Mo, and the $\mathrm{Mo}_{\mathrm{EF}}$:$\mathrm{U}_{\mathrm{EF}}$ ratio declines from ~3 × SW to ~0.3 × SW (i.e., from three times the seawater Mo:U ratio to one-third of that value). EFs generally increase from Zone IV to III to II; Zone I samples do not define a tight cluster but are similar in distribution to Zone III samples. $\mathrm{Mo}_{\mathrm{EF}} - \mathrm{U}_{\mathrm{EF}}$ covariation can provide information about the redox conditions and chemical evolution of a watermass as well as the operation of particulate shuttles (Algeo and Tribovillard, 2009).

5. Discussion

5.1. Contrast between the Hushpuckney Shale Mo isotope record and modern observations

Interpretation of Mo isotope data using modern observations calls for euxinic sediments to have higher δ^{98}Mo values, i.e., closer to the Mo isotopic composition of coeval seawater, than age-equivalent sediments deposited in oxic to weakly euxinic waters (Poulson et al., 2006; Siebert et al., 2006; Poulson Brucker et al., 2009). This reflects the quantitative conversion of molybdate to tetrathiomolybdate and efficient removal of Mo to the sediment in highly euxinic bottom waters (Neubert et al., 2008). Sediments deposited under less reducing conditions have significantly lower δ^{98}Mo values because of isotopic fractionation during Mo removal to the sediment and, hence, do not faithfully record the Mo isotopic composition of contemporaneous seawater

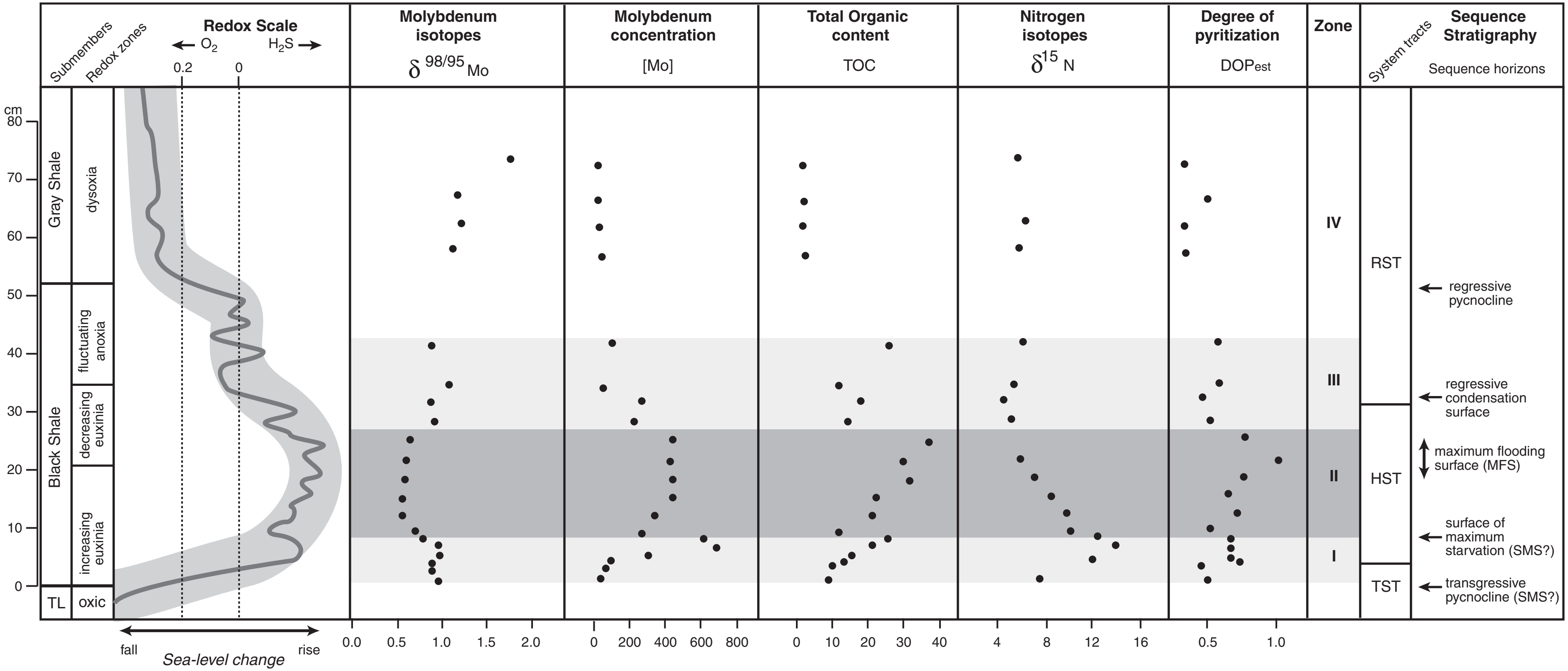

Fig. 2. Geochemical profiles and redox zones through the Hushpuckney Shale in the Edmonds #1A core (modified from Algeo et al., 2004, 2008b). Zones I to III represent the black shale facies and Zone IV represents the gray shale facies of the Hushpuckney Shale. Note that the largest negative shift in δ^{98}Mo is confined to the middle part of the black shale facies (Zone II), which represents the most reducing (i.e., euxinic) conditions as proxied by redox indicators such as DOP_{est}. DOP_{est} is based on a polynomial regression between true DOP (calculated for a subset of samples) and DOP_T (based on total S content; calculated for all samples); see Algeo et al. (2008b) for details.

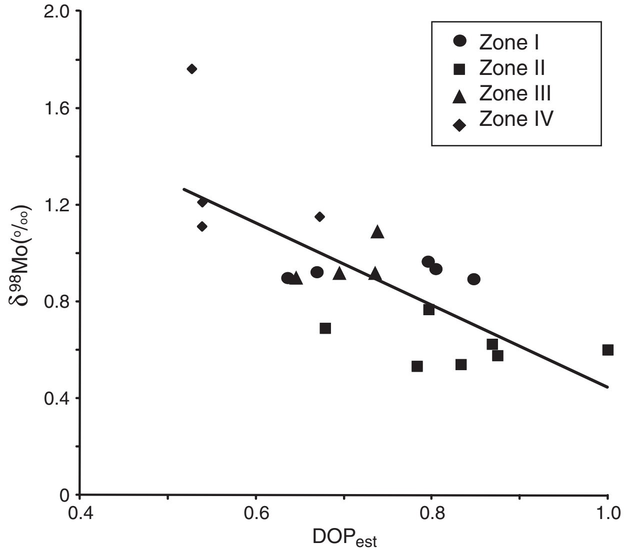

Fig. 3. δ^{98}Mo versus DOP$_{\text{est}}$. Lower δ^{98}Mo values are strongly associated with more reducing conditions (higher DOP$_{\text{est}}$). The correlation coefficient (r) is −0.73, which is significant at $p(\alpha) < 0.001$. Zones I–IV from Fig. 2. See text for further discussion.

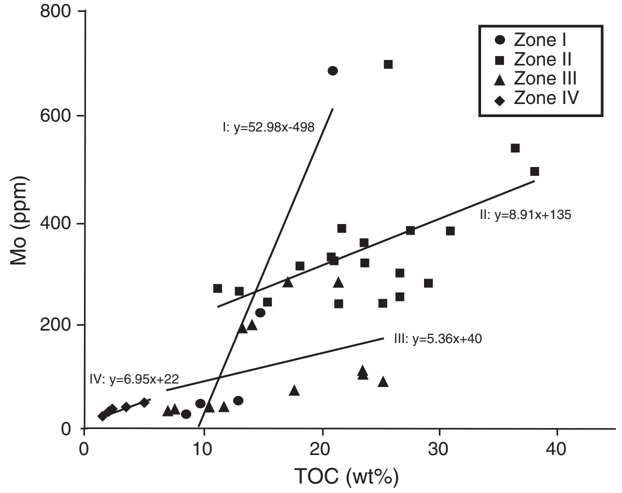

Fig. 5. Total organic carbon (TOC in wt.%) versus molybdenum (Mo) concentrations. Zones from Fig. 2; each zone exhibits a positive correlation for TOC-[Mo] although with differing slopes. The graph includes samples for which no Mo isotope measurements were performed.

(Poulson et al., 2006; Siebert et al., 2006; Poulson Brucker et al., 2009). Fractionation relative to the seawater source of Mo is greater for oxic facies relative to suboxic and most weakly euxinic facies (Poulson et al., 2006; Neubert et al., 2008; Poulson Brucker et al., 2009).

Mo isotopic patterns in the Hushpuckney Shale show surprising relationship with water-column redox conditions (Fig. 7). The most intensely euxinic sediments of Zone II exhibit the lightest δ^{98}Mo values (~+0.6‰), whereas Zone IV, which was deposited under suboxic conditions as shown by geochemical, lithological, and ichnological evidence (Algeo et al., 2004; Algeo and Heckel, 2008), exhibits the heaviest δ^{98}Mo values (~+1.2–1.8‰; Fig. 2). This pattern is the opposite of that for redox facies in the modern Black Sea, in which strongly euxinic sediments of Unit I and oxic sediments of Unit III have δ^{98}Mo values of ~+2.3‰ and ~+0.7‰, respectively (Nägler et al., 2005; Neubert et al., 2008). In addition, Zone II has lighter δ^{98}Mo compared to the less intensely euxinic facies of Zones I and III, whereas the opposite relationship exists between the δ^{98}Mo of strongly and weakly euxinic sediments in the Black Sea. Given that the residence time of seawater within the LPMS was shorter than that in the Black Sea (see Section 1), the euxinic sediments of the former should have recorded the Mo isotopic composition of contemporaneous global seawater. However, the δ^{98}Mo value of the euxinic facies of the Hushpuckney Shale (~+0.6‰) deviates widely from the isotopic composition of modern seawater (+2.3‰; Barling et al., 2001), whereas the δ^{98}Mo values of the suboxic facies (~+1.2–1.8‰) are closer to, but still lower than, that of modern seawater.

Given the shallower water depths and a laterally unconfined basin morphology promoting dynamic watermass exchange, it is likely that the LPMS had dissolved hydrogen sulfide concentrations that were lower than that of the Cariaco Basin (Algeo and Heckel, 2008; Algeo et al., 2008a,b). If $[H_2S]_{aq}$ was indeed low (<11 µM) during deposition of Zone I–III, then it is likely that there was an isotope fractionation during Mo sediment burial such that measured δ^{98}Mo values provide only a minimum estimate of the Mo isotopic composition of contemporaneous seawater, as is the case for organic-rich sediments from weakly euxinic environments in the Baltic Sea, Cariaco Basin, and the shallow Black Sea (<400 m water depth) (Arnold et al., 2004;

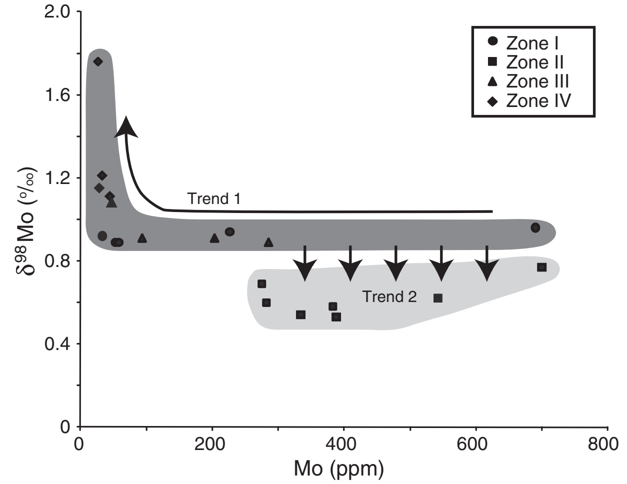

Fig. 4. Mo concentrations versus δ^{98}Mo. Trend 1 represents the "background" relationship, whereas Trend 2 represents a shift toward lower sediment δ^{98}Mo as a consequence of either fractionation related to a local Mn-particulate shuttle or a shift toward a higher anoxic:oxic Mo sink ratio associated with widespread development of euxinic facies. Zones I–IV from Fig. 2.

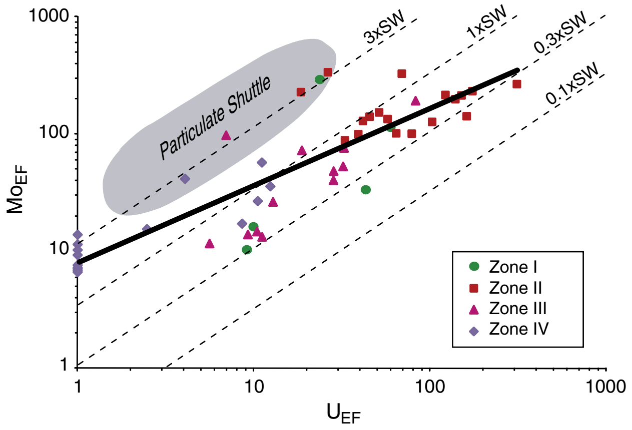

Fig. 6. Mo$_{\text{EF}}$–U$_{\text{EF}}$ covariation. The degree of authigenic enrichment of Mo and U are evaluated using enrichment factors (EF): $X_{EF} = [(X/Al)_{sample}/(X/Al)_{PAAS}]$, where X and Al represent the weight concentrations of element X and Al, respectively, and PAAS is the post-Archean average shale composition of Taylor and McLennan (1985). The dashed diagonal lines represent 3.0, 1.0, 0.3, and 0.1 times the seawater (SW) ratio of Mo to U, and the solid diagonal line represents the correlation for sediment Mo-U in the study unit. Particulate shuttle field from Algeo and Tribovillard (2009) and Tribovillard et al. (2011).

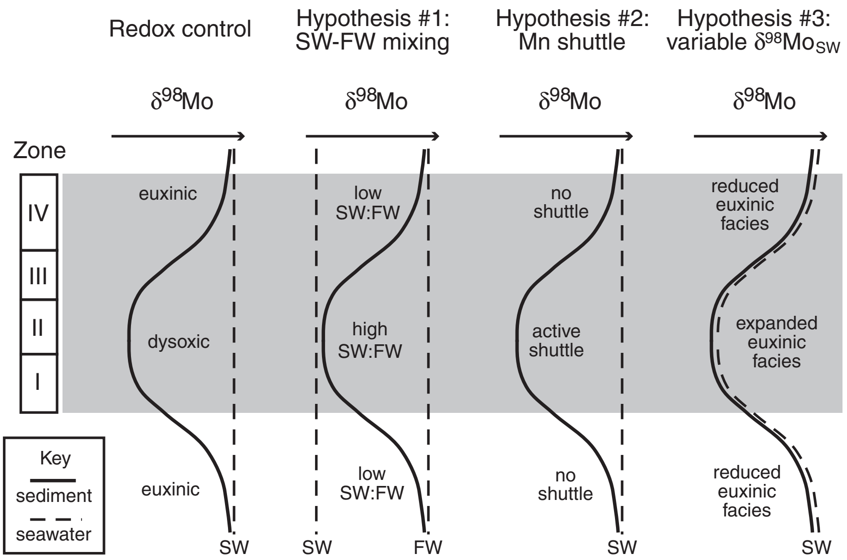

Fig. 7. Generalized patterns of Mo isotopic variation as a function of a simple redox control and the three hypotheses evaluated in the text. Sediment δ^{98}Mo is represented by the solid curve; seawater (SW) and freshwater (FW) δ^{98}Mo by the dashed lines; aqueous δ^{98}Mo values are invariant for all scenarios except #3, in which seawater δ^{98}Mo varies in concert with sediment δ^{98}Mo at time scales associated with deposition of the study unit (~100 kyr). Molybdenum isotope values for each plot increase to the right. See text for discussion.

Neubert et al., 2008; Nägler et al., 2011). A similar pattern of light Mo isotopes during the deposition of organic-rich shales was also observed in one of the Miocene sapropels of the Mediterranean by Scheiderich et al. (2010a), who suggested that sulfide-dependent fractionation of Mo occurred during sapropel deposition. In their model, the depositional environment of the sapropels lacked persistently high $[H_2S]_{aq}$, hampering the full conversion of molybdate to tetrathiomolybdate due to slow reaction kinetics (Erickson and Helz, 2000; Dahl et al., 2010a) and leading to an expression of Mo isotope fractionation between the water column and the sediment.

We evaluate three hypotheses to account for the unusual relationship of δ^{98}Mo values to redox variation in the Hushpuckney Shale.

5.2. Hypothesis #1: control of sediment δ^{98}Mo via riverine influence

If Late Pennsylvanian seawater had a temporally invariant Mo isotopic composition close to that of the euxinic facies of Zone II (~+0.6‰), then some additional process must have been responsible for the heavier δ^{98}Mo values of the suboxic facies of Zone IV, e.g., riverine inputs (Fig. 7). In the modern world, river waters have an average δ^{98}Mo of ~+0.7‰ (Archer and Vance, 2008), although the Mo isotopic composition of freshwater can vary regionally, with values being locally as enriched as +2.3‰ (Hannah et al., 2007; Archer and Vance, 2008; Dahl et al., 2010a; Neubert et al., 2011). Further, the Mo content of river water can vary at short (e.g., annual) time scales, as in the modern Nile River where Mo concentrations rise and δ^{98}Mo values become lighter during the wet season in response to increased chemical weathering (Archer and Vance, 2008).

One possibility is that the low Mo concentrations and high δ^{98}Mo values of Zone IV were due to greater input of isotopically heavy freshwaters into the LPMS (Fig. 7). This hypothesis is consistent with expected changes in seawater:freshwater mixing ratios as a consequence of known patterns of eustatic variation during cyclothem deposition (Fig. 8). Highstand conditions (as during the deposition of Zone II) should lead to maximum seawater:freshwater mixing ratios in the deep watermass owing to greater water depths and upward displacement of the low-salinity surface layer. Conversely, as sea level falls, the influence of the surface layer on sediment composition at a given site will become more pronounced.

The most compelling argument against seawater–freshwater mixing as a dominant control on sediment δ^{98}Mo is related to mixing ratios. Assuming typical concentrations for Mo in seawater (105 nM; Collier, 1985) and freshwater (~6 nM; Archer and Vance, 2008), a simple mass balance calculation shows an exceedingly large volume of freshwater would be required to shift the Mo isotopic composition from +0.6‰ (i.e., the inferred Late Pennsylvanian seawater value based on Zone II results) to +1.8‰ (i.e., the composition of the suboxic facies of Zone IV). For example, if riverine δ^{98}Mo was +2.0‰,

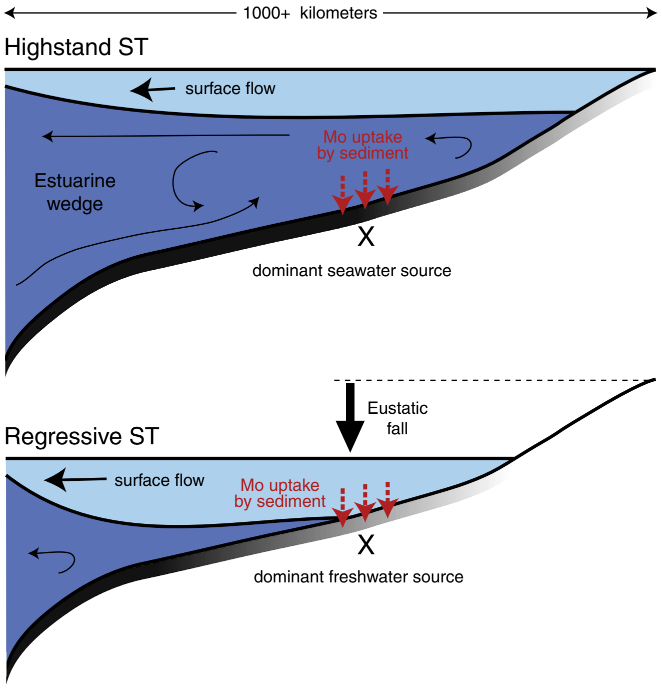

Fig. 8. Hypothesis #1: control of sediment δ^{98}Mo by mixing of seawater and freshwater of differing Mo isotopic compositions. X represents the location of the study unit.

then the seawater:freshwater mixing ratio would have to be 1:100 to achieve a sediment δ^{98}Mo of +1.8‰. Although lowering the Mo concentration of seawater would help, an 80% reduction (i.e., to 20 nM) still requires a 1:20 mixing ratio. If one further assumes a riverine δ^{98}Mo value of +3.0‰ (which is higher than known freshwater sources), an elevated seawater:freshwater mixing ratio (~1:3) is still required to achieve the target sediment δ^{98}Mo value. In essence, no realistic combination of parameters can produce a sediment δ^{98}Mo of +1.8‰ through seawater–freshwater mixing if $\delta^{98}Mo_{sw}$ was as low as +0.6‰ during the Late Pennsylvanian. These findings are consistent with the observation that unambiguous riverine influence on the δ^{98}Mo composition of modern Black Sea sediments is observed only in limnic and strongly brackish facies (Nägler et al., 2005), whereas the marine euxinic facies, deposited in a more restricted setting than the LPMS, records global seawater δ^{98}Mo (Barling et al., 2001; Arnold et al., 2004; Neubert et al., 2008). We conclude that the seawater–freshwater mixing model is not a viable explanation for observed δ^{98}Mo patterns in the Hushpuckney Shale.

5.3. Hypothesis #2: control of sediment δ^{98}Mo via Mn-redox cycling

Another possibility is that Late Pennsylvanian seawater had an invariant and isotopically heavy Mo isotopic composition, i.e., at least +1.8‰, which is the heaviest measured value in the study section (Fig. 7). If the suboxic sediments of Zone IV took up Mo with a small negative fractionation, as is typical of this redox facies (Poulson et al., 2006; Poulson Brucker et al., 2009), then the Mo isotopic composition of Late Pennsylvanian seawater may have been closer to that of modern seawater, i.e., +2.3‰. In this scenario, the light δ^{98}Mo values of Zone II (~+0.6‰) are fractionated relative to coeval seawater. Hence, an additional process must be invoked to achieve the observed pattern of δ^{98}Mo values (Fig. 2).

One such process is Mn-redox cycling, in which solid-phase manganese oxyhydroxide particulates form along the chemocline, where upward-diffusing Mn^{+2} comes into contact with dissolved oxygen, and subsequently scavenge molybdate ions while sinking through the anoxic deeper part of the water column (Fig. 9; Berrang and Grill, 1974; Helz et al., 1996; Zheng et al., 2000; Reitz et al., 2007). The ultimate disposition of this adsorbed Mo depends on the fate of the host particles: where these particles are reductively dissolved, the absorbed Mo is released back into the water column, but where they are carried to the sediment–water interface, the absorbed Mo accumulates in the sediment (Crusius et al., 1996; Algeo and Tribovillard, 2009). Although reductive dissolution of Mn particles may occur following burial, most of the Mo released below the sediment–water interface is scavenged by organic matter or authigenic phases (e.g., Fe sulfide minerals), with only a limited diffusive flux back into the water column (McManus et al., 2006; Helz et al., 2011). However, more complex patterns of Mo recycling within marine sediments may occur under fluctuating redox conditions during diagenesis, leading to additional fractionation of Mo isotopes (Reitz et al., 2007).

The Mn-redox cycling process is capable of accounting for patterns of Mo isotopic variation in modern anoxic marine systems. Reductive dissolution of Mn particles during sinking causes the isotopically light adsorbed Mo to be released back into the water column, leaving no isotopic signature in the sediment. This is the case for the strongly euxinic deep Black Sea (~300–400 μM H_2S), in which abyssal sediments yield δ^{98}Mo values identical to those of the seawater source (Barling et al., 2001; Arnold et al., 2004). On the other hand, survival of a large fraction of sinking Mn particles to the sediment–water interface can impart a light Mo isotopic composition to the sediment. This is the case for the weakly euxinic Cariaco Basin (~50–100 μM H_2S), in which a strong Mn particulate shuttle delivers Mo the seafloor (Algeo and Tribovillard, 2009) and sediment δ^{98}Mo is ~0.5‰ lighter than its seawater source (Arnold et al., 2004). However, these values are substantially less than the ~3‰ negative fractionation associated with molybdate scavenging by deep-ocean Mn-oxide nodules (Barling and Anbar, 2004).

Mo isotopic fractionation associated with Mn-redox cycling can account for the lighter δ^{98}Mo values of Zone II (~+0.6‰) relative to Zone IV (+1.8‰) of the Hushpuckney Shale (Fig. 2). This ~1.2‰ negative fractionation represents a minimum estimate as suboxic sediments are generally somewhat isotopically depleted relative to the seawater source of Mo (Poulson et al., 2006; Siebert et al., 2006; Poulson Brucker et al., 2009). Mo isotope fractionation in the LPMS was thus greater than that in the modern Cariaco Basin (−0.5‰; Arnold et al., 2004) but more similar to that in Lake Cadagno (−1.0 ± 0.2‰; Dahl et al., 2010a). Variations in Mo isotope fractionation may be related to differences in water depth and aqueous hydrogen sulfide concentrations. Water depths in the LPMS were mostly <100 m (Wells et al., 2007; Algeo et al., 2008a) and, hence, closer to those of Lake Cadagno (21 m) than those of the Cariaco Basin (>1400 m). The shallower water depth would have allowed a larger fraction of sinking Mn particles to escape reductive dissolution. Differences in hydrogen sulfide concentrations may have been important as well: although deepwater [H_2S] in the LPMS cannot be determined, it is unlikely to have been as high as in the Cariaco Basin owing to shallower water depths and a laterally unconfined basin morphology that promoted more dynamic watermass exchange (Algeo and Heckel, 2008; Algeo et al., 2008a). Lower deepwater [H_2S] coupled with the shallow-water depth would have reduced the rate of reductive dissolution of Mn particles, allowing more adsorbed Mo to reach the sediment water interface.

Circumstantial evidence for the operation of a Mn-particulate shuttle in the LPMS during deposition of the Hushpuckney Shale is provided by Mo-U concentration data (Fig. 6). Whereas authigenic Mo is strongly enriched in anoxic facies in which a shuttle is active, U is not because it does not adsorb readily onto Mn-OOH particles. Algeo and Tribovillard (2009) documented examples of both modern (Cariaco and Orca basins) and ancient (Late Devonian Appalachian Basin) marine systems in which particulate shuttles accelerated the transfer of aqueous Mo to the sediment. Their results for the LPMS were less clear, but some samples fall within the "particulate shuttle" field (Fig. 6), suggesting that this process may have operated within some areas of the LPMS on at least a transient basis. In a large interior cratonic sea such as the LPMS, the operation of a Mn-redox cycle must have been spatially limited (cf. Berrang and Grill, 1974). In the LPMS, Mn-redox cycling is likely to have operated most vigorously at greater water depths and stronger vertical redox gradients (Fig. 9). These conditions were met during Late Pennsylvanian glacio-eustatic highstands primarily in middle to distal portions of the Midcontinent Shelf, including the present study site. As sea level began to fall during deposition of Zones III and IV of the Hushpuckney Shale (i.e., above the MFS; Fig. 2), water depths became shallower and the vertical redox gradient lessened, producing conditions that eventually terminated operation of the Mn-redox cycle (Fig. 9).

The scenario above, which invokes local control of sediment δ^{98}Mo by Mn-redox cycling, is testable by examining Mo isotopic variation in correlative sections of the Hushpuckney Shale across the LPMS and its relationship to evidence for a particulate shuttle in the form of Mo-U covariation patterns (see Algeo and Tribovillard, 2009). Assuming Mo isotopic variation in the study unit was controlled largely by Mn-redox cycling, we predict that sediment δ^{98}Mo will show substantial spatial variation across the LPMS, with areas of intense Mn-particulate settling characterized by relatively ^{98}Mo-depleted compositions. If further work verifies the influence of Mn-redox cycling on sediment δ^{98}Mo in the LPMS, this observation would have important implications for the use of the Mo isotopic compositions of euxinic sediments as a proxy for $\delta^{98}Mo_{sw}$. Specifically, this process may lead to large and variable degrees of fractionation of Mo isotopes relative to the seawater source, making euxinic shales deposited in regions of active Mn cycling unreliable recorders of contemporaneous global seawater δ^{98}Mo

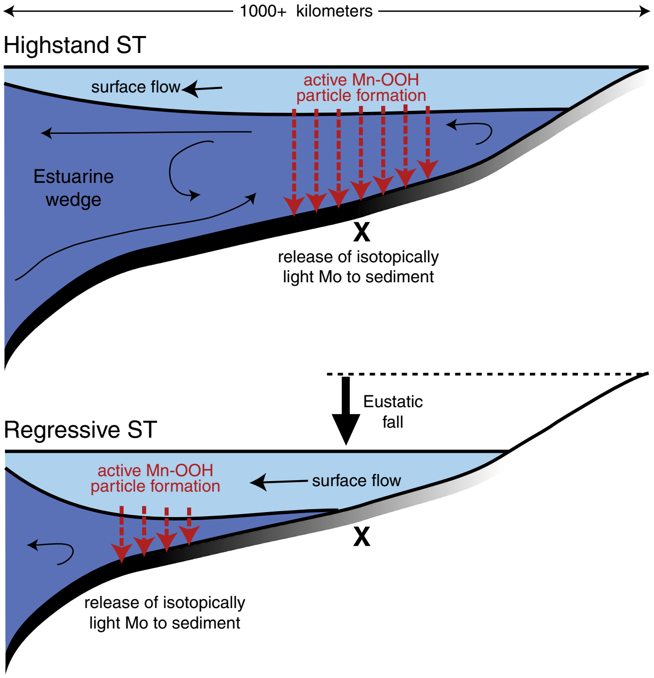

Fig. 9. Hypothesis #2: control of sediment δ^{98}Mo by a water-column Mn-OOH shuttle. X represents the location of the study unit.

(Fig. 7). However, it may be possible to identify those euxinic shales affected by Mn cycling via their δ^{98}Mo values and Mo-U covariation patterns.

5.4. Hypothesis #3: control of sediment δ^{98}Mo via global seawater isotopic changes

The first two hypotheses assumed that $\delta^{98}Mo_{sw}$ remained constant during deposition of the Hushpuckney Shale. However, it is possible that large secular variations in global $\delta^{98}Mo_{sw}$ occurred during the Late Pennsylvanian (Fig. 7) in response to changes in the extent of ocean anoxia. If this process was the dominant control on the Mo isotopic composition of the study unit, then $\delta^{98}Mo_{sw}$ must have varied from ~+0.6‰ during deposition of Zone II (assuming quantitative uptake of Mo by a strongly euxinic facies) to >+1.8‰ during deposition of Zone IV ($\delta^{98}Mo_{sw}$ was likely higher because isotope fractionation occurs during Mo burial in sediments beneath suboxic waters). Thus, the Mo isotopic composition of Late Pennsylvanian seawater would have varied by at least 1.2‰ at the timescales associated with the deposition of individual cyclothemic core shales (~100 kyr; Algeo and Heckel, 2008; Heckel, 2008; Fig. 7). Such rapid changes in the Mo isotope composition of Late Pennsylvanian seawater would have been possible only if seawater Mo concentrations were much lower and seawater Mo residence times were much shorter than those of the modern ocean.

Recent studies have shown that the concentrations and residence times of trace metals in ancient seawater can be estimated from trace metal–TOC relationships in the sediment. For example, Mo/TOC ratios in modern silled anoxic marine basins decrease systematically from ~45 to 4.5 ppm/wt.% with greater watermass restriction and lower aqueous Mo concentrations (Algeo and Lyons, 2006; Algeo and Rowe, 2012). In systems at equilibrium, aqueous trace-metal concentrations are directly proportional to residence time, e.g., a 90% reduction in concentration yields a similar reduction in residence time (Algeo, 2004). These relationships can be used to estimate changes in the trace-metal inventories of paleomarine systems (e.g., Algeo et al., 2007; McArthur et al., 2008; Rowe et al., 2008; Hetzel et al., 2009). Here, we use Mo/TOC ratios to provide a framework for evaluating the Mo isotope record of the Hushpuckney Shale and for comparison with modern settings upon which the Mo isotope paleoredox proxy is based.

Stratigraphic variation in the Mo/TOC ratios of the Hushpuckney Shale (Fig. 5) can be interpreted in terms of secular changes in the Mo inventory of LPMS deepwaters. The Mo/TOC ratio of Zone I (~50 ppm/wt.%) is similar to that of modern euxinic marine facies with nearly unrestricted deepwater exchange (Algeo and Lyons, 2006) as well as to the upper range of Mo/TOC values observed in Phanerozoic euxinic marine sediments (Algeo et al., 2007; Scott et al., 2008). These observations suggest that LPMS deep waters were sourced mainly through advection of open-ocean seawater with little admixture of freshwater during Zone I (Algeo and Maynard, 2008; Algeo et al., 2008a).

The lower Mo/TOC ratios of Zones II and III (~9 and 5 ppm/wt.%, respectively) imply a major change in seawater composition or environmental conditions within the LPMS. These changes in Mo/TOC ratios cannot be attributed to a local redox control, because Zone III yields (1) similar DOP_{est} values to Zone I despite large differences in Mo/TOC, and (2) lower DOP_{est} values than Zone II despite similar Mo/TOC values (Figs. 3 and 5). Lower Mo/TOC ratios also cannot be attributed to freshwater admixture, because seawater:freshwater mixing ratios of <1:4 would have been required to reduce deepwater Mo concentrations sufficiently, and such low mixing ratios are inconsistent with the "normal-marine" character of the benthic fauna in Late Pennsylvanian cyclothems (Heckel, 1977). The lower Mo/TOC ratios of Zones II and III are thus likely to record changes in the aqueous Mo inventory of seawater itself (Fig. 10). Although Algeo and Maynard (2008) presented trace-metal evidence in favor of unrestricted exchange of LPMS deepwaters with the global ocean, it is possible that LPMS deepwaters were in fact moderately restricted. Such restriction may have developed due not to a sill or physical barrier (which probably did not exist; Algeo et al., 2008a,b) but, rather, to the immense distances across the LPMS (>1000 km) over which Mo would have been removed to the sediment and, thus, drawn down in the euxinic deep watermass. Alternatively, the reduced Mo/TOC ratios of Zones II and III might record a whole-ocean drawdown of aqueous Mo concentrations as a consequence of greatly expanded areas of euxinic sedimentation during the transgressive stage of the Swope Formation cyclothem (cf. Algeo, 2004). Whereas the former scenario predicts that Mo/TOC

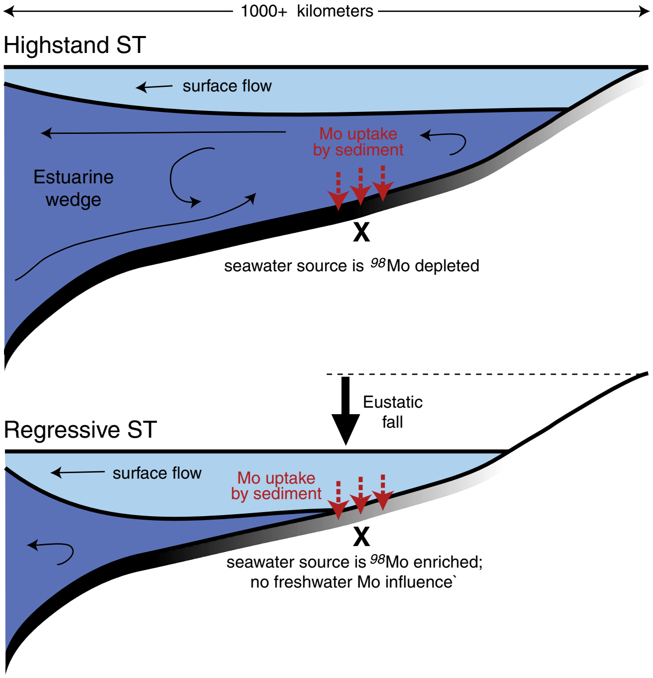

Fig. 10. Hypothesis #3: control of sediment δ^{98}Mo by large short-term changes in the Mo isotopic composition of global seawater. X represents the location of the study unit.

ratios declined from distal to proximal regions of the LPMS, the latter scenario implies spatially uniform Mo/TOC ratios. Thus, these scenarios potentially can be vetted through analysis of spatial variation in Mo/TOC ratios across the LPMS.

By the time of deposition of the suboxic gray shales of Zone IV, the study site was located within the pycnocline separating the anoxic deep watermass from the oxygenated surface watermass (Fig. 10; Heckel, 1977). The latter had a large component of continental runoff (Algeo et al., 2004, 2008a) characterized by a low Mo concentration (cf. ~6 nM for modern rivers; Archer and Vance, 2008), so the Mo content of the surface water layer of the LPMS was reduced in proportion to the admixture of freshwater. Algeo et al. (2008a) estimated the salinity of the surface watermass at 23–27‰, relative to an open-ocean salinity of ~45–50‰ for Late Pennsylvanian seawater, yielding a freshwater:seawater mixing ratio of ~1:1during gray shale deposition. Thus, freshwater inputs would have caused, at most, a 50% reduction in the Mo/TOC ratio of Zone IV relative to Zones I to III. Since the Mo/TOC ratio of Zone IV is not significantly different from that of Zones II and III, differences in Mo concentrations between the deep and surface watermasses of the LPMS may not have been large. The strong reduction in authigenic Mo and TOC enrichment in Zone IV is, rather, a reflection of the suboxic conditions that prevailed during its deposition.

Changes in $\delta^{98}Mo_{sw}$ may have occurred during the Late Pennsylvanian in response to expansion of the area of anoxic marine sedimentation during glacio-eustatic highstands of the Late Paleozoic Ice Age (Fig. 10). Simultaneous flooding of cratons in North America, central Europe, Russia, and elsewhere are known to have generated oxygen-depleted conditions over vast areas (Heckel et al., 2007), even though contemporaneous open-ocean anoxia is unlikely in view of the icehouse climate and high atmospheric O_2 levels of the Pennsylvanian (Otto-Bliesner, 1993; Berner, 1999). A consequent large increase in the anoxic:oxic Mo burial sink ratio (i.e., the proportion of Mo accumulating in anoxic versus oxic facies) may have shifted the isotopic composition of seawater δ^{98}Mo toward lighter compositions (Barling et al., 2001; Arnold et al., 2004; Poulson et al., 2006). In this scenario, such conditions prevailed until sea level began to fall (i.e., above the MFS), at which point a decrease in the area of anoxic marine sedimentation caused $\delta^{98}Mo_{sw}$ to shift back toward heavier compositions (Fig. 10).

This hypothesis is consistent with the sensitive nature of the oceanic Mo mass balance with respect to the areal extent of euxinic bottom waters. Mo burial fluxes are 2–3 orders of magnitude higher in the presence of H_2S compared to O_2. Consequently, sediments deposited beneath suboxic and euxinic waters in the modern oceans comprise ~50–65% of the seawater Mo sink despite the overwhelming preponderance of oxic seafloor (Scott et al., 2008; Kendall et al., 2009; Poulson Brucker et al., 2009; Dahl et al., 2010a; Kendall et al., 2011). Models of the Mo isotope and elemental mass balance require euxinic bottom waters to exist across only a few percent of the seafloor in order to achieve Proterozoic-like seawater Mo concentrations (~5–20 nM based on Mo/TOC data; Scott et al., 2008) and δ^{98}Mo values (~+1‰) (Dahl et al., 2011). Hence, a widespread expansion of shallow epicontinental ocean anoxia during a relatively brief interval (i.e., ≤100 kyr) could have altered the Mo concentration and isotopic composition of global seawater. However, approximately a 85–90% reduction in the concentration of Mo in Late Pennsylvanian seawater would have been necessary in order for the residence time of Mo to have decreased to <100 kyr, i.e., the time scale required for rapid changes in $\delta^{98}Mo_{sw}$ during core shale deposition.

Widespread epicontinental shallow-marine anoxia is likely to result in a reduced oceanic inventory and a shorter residence time of Mo in seawater. Accordingly, the rapid changes in δ^{98}Mo observed in the Hushpuckney Shale (Fig. 2) may not be incompatible with this hypothesis. The Mo/TOC ratios of ~9 ppm/wt.% for Zone II and 5 ppm/wt.% for Zone III are not substantially from the Proterozoic average of 6.4 ppm/wt.%, suggesting that the residence time of Mo in Late Pennsylvanian seawater may have been substantially shorter than that of Mo in modern seawater. Recent modeling of the seawater Mo concentration and residence time in response to increased ocean anoxia (using the conventional modern Mo residence time of ~730 kyr as a starting point) suggests that seawater Mo concentrations of <15 nM can be associated with residence times <100 kyr (Dahl et al., 2011). Using the recent lower estimate of ~440 kyr (Miller et al., 2011) for the modern Mo residence time would permit seawater Mo concentrations of <20 nM at residence times of <100 kyr. A residence time shorter than the estimated accumulation interval of the Hushpuckney Shale (~100 kyr) would have permitted variations in seawater δ^{98}Mo that were then recorded by the sediment. This scenario may account for the different relationships of δ^{98}Mo to Mo concentrations observed in Zone II (Trend 2) relative to the remainder of the study unit (Trend 1; Fig. 4).

Because significant isotope fractionations can occur between seawater and sediments in weakly euxinic environments (from ~0.5‰ in the Cariaco Basin to >2‰ in the Black Sea and Baltic Sea; Arnold et al., 2004; Neubert et al., 2008; Nägler et al., 2011), the extent of anoxic marine sedimentation could have been substantially smaller than implied by the light δ^{98}Mo values of Zone II. It then follows that the magnitude of any redox-driven variations in global seawater δ^{98}Mo arising from glacio-eustatic forcing were modest. Hence, the seawater Mo concentration and residence time during Late Pennsylvanian sea-level highstands need not have been dramatically lower than that of the modern ocean.

The scenario above, which invokes a global control on sediment δ^{98}Mo (i.e., via changes in seawater δ^{98}Mo), is testable by examining Mo isotopic variation (1) in correlative sections of the Hushpuckney Shale across the LPMS (Algeo and Maynard, 1997), and (2) in Late Pennsylvanian cyclothems in other regions such as eastern Europe (Heckel et al., 2007). The same pattern of δ^{98}Mo variation (i.e., a minimum within the early highstand stage) and approximately the same absolute values should be encountered in vertical profile at all locales both within the LPMS and globally. Uniformity of pattern and values is to be expected if secular variation in the Mo isotopic composition of global seawater was the dominant control on sediment δ^{98}Mo. On the other hand, strong local or regional variation in Mo isotope profiles would favor local effects, as imparted by water-column particulate shuttles (i.e., hypothesis #2).

6. Conclusions

Mo abundance and isotope data track changes in aqueous Mo concentrations and redox conditions in the water column of the North American Midcontinent Sea during Late Pennsylvanian transgressive–regressive glacio-eustatic cycles. However, interpreting the Mo isotope record from a single section presents challenges. Using the traditional approach of interpreting changes in Mo isotopes as a proxy for large-scale changes of the Mo budget of the global oceans, our data suggests that the Mo isotope system is sensitive to redox conditions in shallow epicontinental seas, rather than the open oceans, when the open oceans were oxygenated during the Phanerozoic. Changes in the molybdenum isotopic composition of epicontinental black shales could be used to reconstruct the extent of shallow ocean anoxia in epicontinental seas during glacial–interglacial cycles. Alternatively, the Mo isotope record may have been influenced by a strong Mn-oxyhydroxide shuttle in the very shallow, yet large, epicontinental sea. In this case, Mo isotope record would not be a useful proxy for tracking large-scale global changes of the Mo budget or oxygenation history of the Paleozoic. To further test the different models and evaluate if the Mo isotope redox proxy can find application as a tracer of the global extent of shallow anoxia in epicontinental settings, data covering a larger stratigraphic and geographic range are needed in order to identify the major controls on cyclothemic black shales.

Supplementary data to this article can be found online at http://dx.doi.org/10.1016/j.chemgeo.2012.05.013.

Acknowledgments

We thank Lynn Watney and the Kansas Geological Survey for core samples. The project was supported by NSF grant EAR-1052988 to ADH and TJA, and by a grant from the Sol and Esther Drescher Faculty Development Fund (administered through the Barrett Honors College at ASU) to ADH. BK was supported by the NSF Geobiology and Low Temperature Geochemistry and Global Change programs and by the Agouron Institute.

References

Algeo, T.J., 2004. Can marine anoxic events draw down the trace element inventory of seawater? Geology 32, 1057–1060.

Algeo, T.J., Heckel, P.H., 2008. The Late Paleozoic Midcontinent Sea of North America: a review. Palaeogeography, Palaeoclimatology, Palaeoecology 268, 205–221.

Algeo, T.J., Lyons, T., 2006. Mo-total organic carbon covariation in modern anoxic marine environments: Implications for analysis of paleoredox and paleohydrographic conditions. Paleoceanography 21, PA1016 (25 pp.).

Algeo, T.J., Maynard, J.B. (Eds.), 1997. Cyclic Sedimentation of Appalachian Devonian and Midcontinent Pennsylvanian Black Shales: Analysis of Ancient Anoxic Marine Systems—A Combined Core and Field Workshop. Joint Meeting of Eastern Section AAPG and The Society for Organic Petrography (TSOP), Lexington, Kentucky, Sept. 27–28, 1997. 147 pp.

Algeo, T.J., Maynard, J.B., 2004. Trace-element behavior and redox facies in core shales of Upper Pennsylvanian Kansas-type cyclothems. Chemical Geology 206, 298–318.

Algeo, T.J., Maynard, J.B., 2008. Trace metal covariation as a guide to water-mass conditions in ancient anoxic marine environments. Geosphere 4 (5), 872–887.

Algeo, T.J., Rowe, H., 2012. Paleoceanographic applications of trace-metal concentration data. Chemical Geology, this volume.

Algeo, T.J., Tribovillard, N., 2009. Environmental analysis of paleoceanographic systems based on molybdenum–uranium covariation. Chemical Geology 268, 211–225.

Algeo, T.J., Schwark, L., Hower, J.C., 2004. High-resolution geochemistry and sequence stratigraphy of the Hushpuckney Shale (Swope Formation, eastern Kansas): implications for climato-environmental dynamics of the Late Pennsylvanian Midcontinent Seaway. Chemical Geology 206, 259–288.

Algeo, T.J., Lyons, T.W., Blakey, R.C., Over, D.J., 2007. Hydrographic conditions of the Devono-Carboniferous North American Seaway inferred from sedimentary Mo-TOC relationships. Palaeogeography, Palaeoclimatology, Palaeoecology 256, 204–230.

Algeo, T., Rowe, H., Hower, J.C., Schwark, L., Herrmann, A.D., Heckel, P., 2008a. Oceanic denitrification during Late Carboniferous glacial–interglacial cycles. Nature Geoscience 1, 709–714.

Algeo, T.J., Heckel, P.H., Maynard, J.B., Blakey, R.C., Rowe, H., 2008b. Modern and ancient epicratonic seas and the superestuarine circulation model of marine anoxia. In: Holmden, C., Pratt, B.R. (Eds.), Dynamics of Epeiric Seas: Sedimentological, Paleontological and Geochemical Perspectives: Geological Association of Canada Special Publication, 48, pp. 7–38.

Archer, C., Vance, D., 2008. The isotopic signature of the global riverine molybdenum flux and anoxia in the ancient oceans. Nature Geoscience 1, 597–600.

Arnold, G.L., Anbar, A.D., Barling, J., Lyons, T.W., 2004. Molybdenum isotope evidence of widespread anoxia in mid-Proterozoic oceans. Science 304, 87–90.

Arnórsson, S., Óskarsson, N., 2007. Molybdenum and tungsten in volcanic rocks and in surface- and <100°C ground waters in Iceland. Geochimica et Cosmochimica Acta 71, 284–304.

Barling, J., Anbar, A.D., 2004. Molybdenum isotope fractionation during adsorption by manganese oxides. Earth and Planetary Science Letters 217, 315–329.

Barling, J., Arnold, G.L., Anbar, A.D., 2001. Natural mass-dependent variations in the isotopic composition of molybdenum. Earth and Planetary Science Letters 193, 447–457.

Berner, R.A., 1999. Atmospheric oxygen over Phanerozoic time. Proceedings of the National Academy of Sciences U. S. A. 96, 10955–10957.

Berrang, P.G., Grill, E.V., 1974. The effect of manganese oxide scavenging on molybdenum in Saanich Inlet, British Columbia. Marine Chemistry 2, 125–148.

Collier, R.W., 1985. Molybdenum in the northeast Pacific Ocean. Limnology and Oceanography 30, 1351–1353.

Coveney Jr., R.M., Watney, W.L., Maples, C.G., 1991. Contrasting depositional models for Pennsylvanian black shale discerned from molybdenum abundances. Geology 19, 147–150.

Crowley, T.J., Hyde, W.T., Short, D.A., 1989. Seasonal cycle variations on the supercontinent of Pangaea. Geology 17, 457–460.

Crowley, T.J., Yip, K.-J., Baum, S.K., Moore, S.B., 1996. Modelling Carboniferous coal formation. Paleoclimates 2, 159–177.

Cruse, A.M., Lyons, T.W., 2000. Sedimentology and geochemistry of the Hushpuckney and Upper Tackett shales: cyclothem models revisited. Oklahoma Geological Survey Circular 103, 185–194.

Cruse, A.M., Lyons, T.W., 2004. Trace metal records of regional paleoenvironmental variability in Pennsylvanian (Upper Carboniferous) black shales. Chemical Geology 206, 319–345.

Crusius, J., Calvert, S., Pedersen, T., Sage, D., 1996. Rhenium and molybdenum enrichments in sediments as indicators of oxic, suboxic and sulfidic conditions of deposition. Earth and Planetary Science Letters 145, 65–78.

Dahl, T.W., Anbar, A.D., Gordon, G.W., Rosing, M.T., Frei, R., Canfield, D.E., 2010a. The behavior of molybdenum and its isotopes across the chemocline and in the sediments of sulfidic Lake Cadagno, Switzerland. Geochimica et Cosmochimica Acta 74, 144–163.

Dahl, T.W., Hammarlund, E.U., Anbar, A.D., Bond, D.P.G., Gill, B.C., Gordon, G.W., Knoll, A.H., Nielsen, A.T., Schovsbo, N.H., Canfield, D.E., 2010b. Devonian rise in atmospheric oxygen correlated to the radiations of terrestrial plants and large predatory fish. Proceedings of the National Academy of Sciences (U.S.A.) 107, 17911–17915.

Dahl, T.W., Canfield, D.E., Rosing, M.T., Frei, R.E., Gordon, G.W., Knoll, A.H., Anbar, A.D., 2011. Molybdenum evidence for expansive sulfidic water masses in 750 Ma oceans. Earth and Planetary Science Letters 311, 264–274.

Duan, Y., Anbar, A.D., Arnold, G.L., Lyons, T.W., Gordon, G.W., Kendall, B., 2010. Molybdenum isotope evidence for mild environmental oxygenation before the Great Oxidation Event. Geochimica et Cosmochimica Acta 74, 6655–6668.

Erickson, B.E., Helz, G.R., 2000. Molybdenum(VI) speciation in sulfidic waters: stability and lability of thiomolybdates. Geochimica et Cosmochimica Acta 64, 1149–1158.

Gordon, G.W., Lyons, T.W., Arnold, G.L., Roe, J.E., Sageman, B.B., Anbar, A.D., 2009. When do black shales tell molybdenum isotope tales? Geology 37, 535–538.

Greb, S.F., Pashin, J.C., Martino, R.L., Eble, C.F., 2008. Appalachian sedimentary cycles during the Pennsylvanian: Changing influences of sea level, climate, and tectonics. In: Fielding, C.R., Frank, T.D., Isbell, J.L. (Eds.), Resolving the Late Paleozoic Ice Age in Time and Space: Geological Society of America Special Paper, 441, pp. 235–248.

Hannah, J.L., Stein, H.J., Wieser, M.E., de Laeter, J.R., Varner, M.D., 2007. Molybdenum isotope variations in molybdenite: vapor transport and Rayleigh fractionation of Mo. Geology 35, 703–706.

Heckel, P.H., 1977. Origin of phosphatic black shale facies in Pennsylvanian cyclothems of mid-continent North America. Bulletin of the American Association of Petroleum Geologists 61, 1045–1068.

Heckel, P.H., 1986. Sea-level curve for Pennsylvanian eustatic marine transgressive–regressive depositional cycles along midcontinent outcrop belt, North America. Geology 14, 330–334.

Heckel, P.H., 1994. Evaluation of evidence for glacial-eustatic control over marine Pennsylvanian cyclothems in North America and consideration of possible tectonic effects. In: Dennison, J.M., Ettensohn, F.R. (Eds.), Tectonic and Eustatic Controls on Sedimentary Cycles: SEPM-Society for Sedimentary Geology, Concepts in Sedimentology and Paleontology, 4, pp. 65–87.

Heckel, P.H., 2008. Pennsylvanian cyclothems in Midcontinent North America as far-field effects of waxing and waning of Gondwana ice sheets. In: Fielding, C.R., Frank, T.D., Isbell, J.L. (Eds.), Resolving the Late Paleozoic Ice Age in Time and Space: Geological Society of America Special Paper, 441, pp. 275–290.

Heckel, P.H., Alekseev, A.S., Barrick, J.E., Boardman, D.R., Goreva, N.V., Nemyrovska, T.I., Ueno, K., Villa, E., Work, D.M., 2007. Cyclothem ["digital"] correlation and biostratigraphy across the global Moscovian-Kasimovian-Gzhelian stage boundary interval (Middle-Upper Pennsylvanian) in North America and eastern Europe. Geology 35, 607–610.

Helz, G.R., Miller, C.V., Charnock, J.M., Mosslemans, J.F.W., Pattrick, R.A.D., Garner, C.D., Vaughan, D.J., 1996. Mechanism of molybdenum removal from the sea and its concentration in black shales: EXAFS evidence. Geochimica et Cosmochimica Acta 60, 3631–3642.

Helz, G.R., Bura-Nakić, E., Mikac, N., Cigleneçki, I., 2011. New model for molybdenum behavior in euxinic waters. Chemical Geology 284, 323–332.

Hetzel, A., Böttcher, M.E., Wortmann, U.G., Brumsack, H.-J., 2009. Paleo-redox conditions during OAE 2 reflected in Demerara Rise sediment geochemistry (ODP Leg 207). Palaeogeography, Palaeoclimatology, Palaeoecology 273, 302–328.

Hoffman, D.L., Algeo, T.J., Maynard, J.B., Joachimski, M.M., Hower, J.C., Jaminski, J., 1998. Regional and stratigraphic variation in bottomwater anoxia in offshore core shales of Upper Pennsylvanian cyclothems from the Eastern Midcontinent Shelf (Kansas), USA. In: Schieber, J., Zimmerle, W., Sethi, P.S. (Eds.), Shales and Mudstones. Stuttgart, Schweizerbart'sche Verlagsbuchhandlung, pp. 243–269.

Horton, D.E., Poulsen, C.J., 2009. Paradox of late Paleozoic glacioeustasy. Geology 37, 715–718.

Horton, D.E., Poulsen, C.J., Pollard, D., 2010. Influence of high-latitude vegetation feedbacks on late Palaeozoic glacial cycles. Nature Geoscience 3, 572–577.

Joachimski, M.M., von Bitter, P.H., Buggisch, W., 2006. Constraints on Pennsylvanian glacioeustatic sea-level changes using oxygen isotopes of conodont apatite. Geology 34, 277–280.

Kendall, B., Creaser, R.A., Gordon, G.W., Anbar, A.D., 2009. Re-Os and Mo isotope systematics of black shales from the Middle Proterozoic Velkerri and Wollogorang Formations, McArthur Basin, Northern Australia. Geochimica et Cosmochimica Acta 73, 2534–2558.

Kendall, B., Gordon, G.W., Poulton, S.W., Anbar, A.D., 2011. Molybdenum isotope constraints on the extent of late Paleoproterozoic ocean euxinia. Earth and Planetary Science Letters 307, 450–460.

Lehmann, B., Nägler, T.F., Holland, H.D., Wille, M., Mao, J., Pan, J., Ma, D., Dulski, P., 2007. Highly metalliferous carbonaceous shale and Early Cambrian seawater. Geology 35, 403–406.

McArthur, J.M., Algeo, T.J., van de Schootbrugge, B., Li, Q., Howarth, R.J., 2008. Basinal restriction, black shales, and the Early Toarcian (Jurassic) oceanic anoxic event. Paleoceanography 23, PA4217, http://dx.doi.org/10.1029/2008PA001607 (22 pp.).

McLennan, S.M., 2001. Relationships between the trace element composition of sedimentary rocks and upper continental crust. Geochemistry Geophysics Geosystems (G3) 2, GC000109 (24 pp.).

McManus, J., Berelson, W.M., Severmann, S., Poulson, R.L., Hammond, D.E., Klinkhammer, G.P., Holm, C., 2006. Molybdenum and uranium geochemistry in continental margin sediments: paleoproxy potential. Geochimica et Cosmochimica Acta 70, 4643–4662.

Miller, C.A., Peucker-Ehrenbrink, B., Walker, B.D., Marcantonio, F., 2011. Re-assessing the surface cycling of molybdenum and rhenium. Geochimica et Cosmochimica Acta 75, 7146–7179.

Millero, F.J., 1996. Chemical Oceanography, Second ed. CRC Press, Boca Raton, Florida. 469 pp.

Morford, J.L., Emerson, S., 1999. The geochemistry of redox sensitive trace metals in sediments. Geochimica et Cosmochimica Acta 63, 1735–1750.

Nägler, T.F., Siebert, C., Lüschen, H., Böttcher, M.E., 2005. Sedimentary Mo isotope record across the Holocene fresh-brackish water transition of the Black Sea. Chemical Geology 219, 283–295.

Nägler, T.F., Neubert, N., Böttcher, M.E., Dellwig, O., Schnetger, B., 2011. Molybdenum isotope fractionation in pelagic euxinia: evidence from the modern Black and Baltic Seas. Chemical Geology 289, 1–11.

Neubert, N., Nägler, T.F., Böttcher, M.E., 2008. Sulfidity controls molybdenum isotope fractionation in euxinic sediments: evidence from the modern Black Sea. Geology 36, 775–778.

Neubert, N., Heri, A.R., Voegelin, A.R., Nägler, T.F., Schlunegger, F., Villa, I.M., 2011. The molybdenum isotopic composition in river water: constraints from small catchments. Earth and Planetary Science Letters 304, 180–190.

Otto-Bliesner, B.L., 1993. The role of mountains, polar ice, and vegetation in determining the tropical climate during the Middle Pennsylvanian: Climate model simulations. In: Cecil, C.B. (Ed.), Climate Controls on Stratigraphy: SEPM-Society for Sedimentary Geology Special Publication, 77, pp. 227–237.

Pearce, C.R., Cohen, A.S., Coe, A.L., Burton, K.W., 2008. Molybdenum isotope evidence for global ocean anoxia coupled with perturbations to the carbon cycle during the Early Jurassic. Geology 36, 231–234.

Poulsen, C.J., Pollard, D., Montañez, I.P., Rowley, D., 2007. Late Paleozoic tropical climate response to Gondwanan deglaciation. Geology 35, 771–774.

Poulson Brucker, R.L., McManus, J., Severmann, S., Berelson, W.M., 2009. Molybdenum behavior during early diagenesis: insights from Mo isotopes. Geochemistry Geophysics Geosystems (G3) 10, Q0610 (25 pp.).

Poulson, R.L., Siebert, C., McManus, J., Berelson, W.M., 2006. Authigenic molybdenum isotope signatures in marine sediments. Geology 34, 617–620.

Reitz, A., Wille, M., Nägler, T.F., de Lange, G.J., 2007. Atypical Mo isotope signatures in eastern Mediterranean sediments. Chemical Geology 245, 1–8.

Rowe, H.D., Loucks, R.G., Ruppel, S.C., Rimmer, S.M., 2008. Mississippian Barnett Formation, Fort Worth Basin, Texas: bulk geochemical inferences and Mo-TOC constraints on the severity of hydrographic restriction. Chemical Geology 257, 16–25.

Scheiderich, K., Helz, G.R., Walker, R.J., 2010a. Century-long record of Mo isotopic composition in sediments of a seasonally anoxic estuary (Chesapeake Bay). Earth and Planetary Science Letters 289, 189–197.

Scheiderich, K., Zerkle, A.L., Helz, G.R., Farquhar, J., Walker, R.J., 2010b. Molybdenum isotope, multiple sulfur isotope, and redox-sensitive element behavior in early Pleistocene Mediterranean sapropels. Chemical Geology 279, 134–144.

Schultz, R.B., Coveney Jr., R.M., 1992. Time-dependent changes for midcontinent Pennsylvanian black shales, U.S.A. Chemical Geology 99, 83–100.

Schutter, S., Heckel, P.H., 1985. Missourian (early Late Pennsylvanian) climate in Midcontinent North America. International Journal of Coal Geology 5, 111–140.

Scott, C., Lyons, T.W., Bekker, A., Shen, Y., Poulton, S.W., Chu, X., Anbar, A.D., 2008. Tracing the stepwise oxygenation of the Proterozoic ocean. Nature 452, 456–459.

Siebert, C., Nägler, T.F., von Blanckenburg, F., Kramers, J.D., 2003. Molybdenum isotope records as a potential new proxy for paleoceanography. Earth and Planetary Science Letters 211, 159–171.

Siebert, C., McManus, J., Bice, A., Poulson, R., Berelson, W.M., 2006. Molybdenum isotope signatures in continental margin marine sediments. Earth and Science Planetary Letters 241, 723–733.

Taylor, S.R., McLennan, S.M., 1985. The Continental Crust: Its Composition and Evolution. Blackwell, Oxford. 312 pp.

Tribovillard, N., Algeo, T.J., Baudin, F., Riboulleau, A., 2011. Analysis of marine environmental conditions based on molybdenum–uranium covariation—Applications to Mesozoic paleoceanography. Chemical Geology, this volume.

Watney, W.L., French, J.A., Doveton, J.H., Youle, J.C., Guy, W.J., 1995. Cycle hierarchy and genetic stratigraphy of Middle and Upper Pennsylvanian strata in the Upper Midcontinent. In: Hyne, N.J. (Ed.), Sequence Stratigraphy of the Mid-Continent: Geological Society of Tulsa Special Publication, 4, pp. 141–192.

Wells, M.R., Allison, P.A., Piggott, M.D., Gorman, G.J., Hampson, G.J., Pain, C.C., Fang, F., 2007. Numerical modeling of tides in the Late Pennsylvanian Midcontinent Seaway of North America with implications for hydrography and sedimentation. Journal of Sedimentary Research 77, 843–865.

Wille, M., Nägler, T.F., Lehmann, B., Schröder, S., Kramers, J.D., 2008. Hydrogen sulphide release to surface waters at the Precambrian/Cambrian boundary. Nature 453, 767–769.

Zheng, Y., Anderson, R.F., van Geen, A., Kuwabara, J., 2000. Authigenic molybdenum formation in marine sediments: a link to pore water sulfide in the Santa Barbara Basin. Geochimica et Cosmochimica Acta 64, 4165–4178.